COMMUNICATION

Solid-State Structure of Protonated Ketones and Aldehydes

*Daniel Stuart, Stacey D. Wetmore, and Michael Gerken**

In memoriam George A. Olah

Abstract: Protonated carbonyl compounds have been invoked as intermediates in many acid-catalyzed organic reactions. To gain key structural and electronic data about such intermediates, oxonium salts derived from five representative examples of ketones and aldehydes are synthesized in the solid state, and characterized by X-ray crystallography and Raman spectroscopy for the first time. DFT calculations were carried out on the cations in the gas-phase. Whereas an equimolar reaction of the carbonyl compounds, acetone, cyclopentanone, adamantanone, and acetaldehyde, with SbF_5 in anhydrous HF yielded mononuclear oxonium cations, the same stoichiometry in a reaction with benzaldehyde resulted in formation of a hemiprotonated, hydrogen-bridged dimeric cation. Hemiprotonated acetaldehyde was obtained when a 2:1 ratio of aldehyde and SbF_5 was used. Experimental and NBO analyses quantify the significant increase in electrophilicity of the oxonium cations compared to that of the parent ketones/aldehydes.

Protonated ketones and aldehydes are key intermediates in many organic reactions. Ground-breaking work by Gillespie and Olah proved by NMR spectroscopy that these cationic intermediates can be stabilized in superacidic solutions at low temperatures (LT).[1] One of the first ketones to be studied by ^{1}H NMR spectroscopy was the conjugate acid of acetone, with a pKa of −7.3, giving rise to a ^{1}H resonance of the C=OH$^+$ group at 14.45 ppm.[1a] Synthesizing these protonated compounds requires a proton source from a superacidic medium such as HSO_3F-SbF_5 ("magic acid") or HF/SbF_5. Two resonance structures can be written for protonated ketones and aldehydes: the oxonium and hydroxycarbenium cation structures (Scheme 1). The highly deshielded ^{1}H resonances between 13 and 15 ppm,[1b-d] as well as the observation of the *E*- and *Z*-stereoisomers of protonated aldehydes and unsymmetrically substituted ketones.[1c,d] provides strong evidence that the oxonium resonance structure is the primary resonance existing in solution.

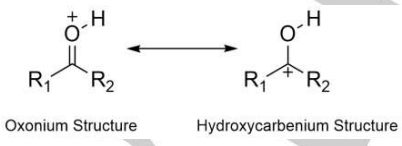

Scheme 1. Resonance structures for protonated ketones.

[*] D. Stuart, Prof. Dr. S. D. Wetmore, Prof. Dr. M. Gerken
Canadian Centre for Research in Advanced Fluorine Technologies and Department of Chemistry and Biochemistry
University of Lethbridge
4401 University Drive, Lethbridge, AB T1K 3M4 (Canada)
E-mail: michael.gerken@uleth.ca

Supporting information for this article is given via a link at the end of the document.((Please delete this text if not appropriate))

A small number of protonated ketones have been studied in the solid state. Structural studies of monoprotonated ketones are limited to a group of cyclopropylcarbinyl derivatives which were part of investigations of the stabilization of a positive charge by cylcopropyl groups and in homoaromatic systems.[2] In one attempt to isolate the 2-hydroxyhomotropylium benzannelated cation, the X-ray crystal structure showcased a hemiprotonated cation consisting of two deuterium-bridged ketones.[3] In a study involving the isolation of solvated protons in organic oxygen-donor solvents, the synthesis and X-ray crystal structure of hemiprotonated benzophenone was determined.[4] Computational studies using the B3LYP/6-31++G(d,p) level of theory have been carried out on the carbonyl bases R_2C=O (R = F, H, CH_3), investigating the changes in bond lengths and vibrational frequencies upon protonation.[5] In addition, semi-empirical studies in conjunction with mass spectrometric measurements have been used to study the geometric properties and stability of protonated acetone clusters.[6]

Currently, no solid-state studies of protonated aldehydes have been reported. Mass spectrometry studies along with quantum-chemical calculations were used to probe protonated benzaldehyde.[7] Excited state and optimized geometry calculations showed the lowest-energy configuration to be the *E*-configuration.[8] Mass spectrometry studies, along with gas-phase calculations, have suggested that formaldehyde and acetaldehyde form hydrogen-bridged dimers, $(RCHO)_2H^+$ (R = H or CH_3).[9] Attempts to synthesize protonated formaldehyde in the solid state have been unsuccessful and instead a $[H_2C$=O−$CH_2OH]^+$ salt was obtained in HF/SbF_5 at −78 °C and characterized by X-ray crystallography, and IR and Raman spectroscopy.[10]

While exploring the interactions of $[SF_3]^+$ with ketones in our studies of the mechanisms of deoxofluorination reactions, an equimolar reaction between $[SF_3][AsF_6]$ and 2-adamantanone (**1**) in anhydrous hydrogen fluoride (aHF) resulted in protonation of the carbonyl group and the synthesis of the $[AsF_6]^-$ salt of $[\mathbf{1}-H]^+$. The protonation of the ketone can be explained by the superacidic nature of the $[SF_3][AsF_6]$/aHF system [Eq. (1)]. When isolating the product, SF_4 is easily removed under dynamic vacuum.

$$[SF_3][AsF_6] + 2HF \rightleftharpoons SF_4 + [H_2F][AsF_6] \quad (1)$$

In targeted reactions, salts of protonated ketones and aldehydes were isolated using stoichiometric amounts of either $[SF_3][AsF_6]$ or SbF_5 in aHF. Reactions using AsF_5 were attempted, but led to inaccurate stoichiometric ratios, which resulted in reduced stability of the product, likely due to oxidation of the organic substrate by excess AsF_5.

Reactions of $[SF_3][AsF_6]$ with **1** and cyclopentanone (**2**) in aHF at −78 °C resulted in the synthesis of the hexafluoroarsenate salts $[\mathbf{1}-H]^+$ and $[\mathbf{2}-H]^+$, respectively, according to Eq. (2). Reaction occurred instantaneously upon melting, producing white powders that dissolved at 0 °C. Crystals of $[\mathbf{1}-H][AsF_6]$ and $[\mathbf{2}-H][AsF_6]$

grew from aHF at −20 °C and −78 °C, respectively. The salt of [**1**−H]$^+$ was stable at room-temperature (RT) for 20 min before turning a pale yellow colour, whereas [**2**−H][AsF_6] was more stable and remained a white powder for upwards of 1 h. The bands in the LT Raman spectra showed no change in frequency; however, increasing fluorescence was observed in the spectral baseline the longer the sample was left at RT.

$$[SF_3][AsF_6] + O{=}R + HF \xrightarrow{aHF} [HO{=}R][AsF_6] + SF_4 \quad (R = C_{10}H_{14}\,(\mathbf{1}),\ C_5H_8\,(\mathbf{2})) \qquad (2)$$

Hexafluoroantimonate salts can be obtained via the reaction of ketones with 1 molar equivalent of SbF_5 in aHF. The reaction of **1**, **2**, and acetone (**3**) with SbF_5 in aHF at −78 °C resulted in immediate reactions producing white powders of [**1**−H][SbF_6], [**2**−H][SbF_6], and [**3**−H][SbF_6], respectively, according to Eq. (3). [**3**−H][SbF_6] proved to be the most stable salt among those studied, lasting 24 h at RT before LT Raman spectroscopy showed some fluorescence in the baseline.

$$SbF_5 + O{=}R + HF \xrightarrow{aHF} [HO{=}R][SbF_6] \quad (R = C_{10}H_{14}\,(\mathbf{1}),\ C_5H_8\,(\mathbf{2}),\ C(CH_3)_2\,(\mathbf{3})) \qquad (3)$$

The crystal structures of [**1**−H][AsF_6], [**2**−H][AsF_6], and [**3**−H][SbF_6] (Figure 1) clearly show the protonation of 2-adamantanone, cyclopentanone, and acetone, which results in an increase in the C=O bond lengths ([**1**−H]$^+$ 1.274(2) Å; [**2**−H]$^+$ 1.266(3); [**3**−H]$^+$ 1.271(3) and 1.273(3) Å) compared to their respective parent ketones (**1** 1.215(3) Å;[11] **2** 1.21909(15) Å;[12] **3** 1.208(3) Å[13]) (Table 1). The C=O bond lengths of the protonated compounds, however, remain significantly shorter than the typical C–O single bond in an alcohol (1.432(13) Å).[14] As confirmed by DFT calculations at the B3LYP/aug-cc-pVTZ level of theory (Table 1), a significant decrease in the $C_{C=O}$–C bond lengths is observed for the protonated ketones ($C_{C=O}$–C_{cis}: [**1**−H]$^+$ 1.469(2) Å; [**2**−H]$^+$ 1.473(3) Å; [**3**−H]$^+$ 1.467(3) Å) relative to the parent compounds (**1** 1.5176(16) Å;[11] **2** 1.5078(18) Å;[12] **3** 1.478(4) Å).[13] Whereas slightly longer $C_{C=O}$–C_{cis} bonds are calculated than for the $C_{C=O}$–C_{trans} bonds, the experimental $C_{C=O}$–C bond distances in each protonated ketone are the same within 3σ. The oxonium cations [**1**−H]$^+$ and [**2**−H]$^+$ in the [AsF_6]$^-$ salts exhibit strong hydrogen bonds to a F atom of the [AsF_6]$^-$ anion. The O---F distance in [**1**−H]$^+$ (O---F(1) 2.6233(16) Å) is larger than [**2**−H]$^+$ (O---F(1) 2.560(3) Å), however, both are comparable to previously reported hydrogen bonds in protonated cyclopropylcarbinyl derivates (O---F 2.557(6) and 2.601(6) Å).[2d] These hydrogen bonds result in an elongation of the As–F(1) distance and an ensuing distortion of the idealized octahedral geometry of the anion. The [**2**−H][AsF_6] and [**2**−H][SbF_6] salts are isostructural with cation [**2**−H]$^+$ in both salts exhibiting no difference in the C=O bond length (1.267(2) Å). The [AsF_6]$^-$ salt, however, forms stronger hydrogen-bonding interactions (O---F(1) 2.560(3) Å) than in the [SbF_6]$^-$ salt (O---F(1) 2.6043(16) Å). Unlike [**1**−H]$^+$ and [**2**−H]$^+$ salts, the X-ray crystal structure of [**3**−H][SbF_6] crystallized in the $P\bar{1}$ space group with two crystallographically unique cations and three different anion environments in the unit cell. One of the three [SbF_6]$^-$ anions does not have any significant contacts with the oxonium cation, whereas the other two anions accept one or two hydrogen-bonds from [**3**−H]$^+$ cations.

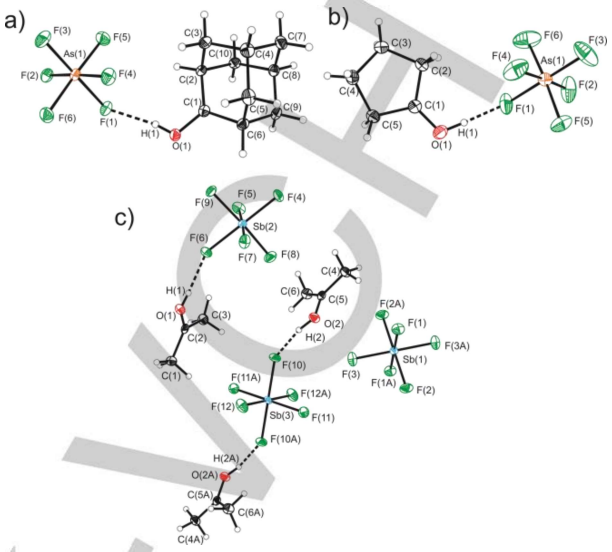

Figure 1. Thermal ellipsoid plots of a) [**1**−H][AsF_6], b) [**2**−H][AsF_6], c) [**3**−H][SbF_6]. Thermal ellipsoids are set at the 50% probability level.

Table 1. Selected Experimental and Calculated Bond Lengths (Å) of Oxonium Cations [**1**−H]$^+$, [**2**−H]$^+$, and [**3**−H]$^+$ as well as the Parent Ketones 2-Adamantanone (**1**), Cyclopentanone (**2**), and Acetone (**3**).

	1		[**1**−H]$^+$	
	exptl [b]	*calcd* [e]	*exptl*	*calcd* [e]
C=O	1.215(3)	1.213	1.274(2)	1.285
$C_{C=O}$–C_{cis} [a]	1.5176(16)	1.524	1.469(2)	1.468
$C_{C=O}$–C_{trans} [a]	1.5176(16)	1.524	1.472(2)	1.464
O---F			2.6233(16)	
	2		[**2**−H]$^+$	
	exptl [c]	*calcd* [e]	*exptl* $[AsF_6]^-$; $[SbF_6]^-$	*calcd* [e]
C=O	1.2109(15) 1.2148(15)	1.205	1.266(3); 1.267(2)	1.275
$C_{C=O}$–C_{cis} [a]	1.5078(18) 1.5103(14)	1.528	1.473(3); 1.481(2)	1.476
$C_{C=O}$–C_{trans} [a]	1.5111(15) 1.5103(14)	1.528	1.469(3); 1.477(2)	1.470
O---F			2.560(3); 2.6043(16)	
	3		[**3**−H]$^+$	
	exptl [d]	*calcd* [e]	*exptl*	*calcd* [e]
C=O	1.208(3) 1.209(3)	1.210	1.271(3) O(1)−C(2) 1.273(3) O(2)−C(5)	1.277
$C_{C=O}$–C_{cis} [a]	1.478(4) 1.485(4)	1.514	1.467(3) C(2)−C(3) 1.469(4) C(5)−C(6)	1.470
$C_{C=O}$–C_{trans} [a]	1.485(4) 1.486(4)	1.514	1.459(4) C(1)−C(2) 1.464(4) C(4)−C(5)	1.466
O---F			2.597(2) 2.619(2)	

[a] Refers to the carbon *cis* or *trans* to the proton on the oxygen. [b] from Ref. 11; [c] from Ref. 12; [d] from Ref. 13; [e] DFT calculations at the B3LYP/aug-cc-pVTZ level of theory.

The DFT-optimized gas-phase geometries of the oxonium cations [**1**–H]$^+$, [**2**–H]$^+$, and [**3**–H]$^+$, as well as their parent ketones, generally show excellent agreement with the experimental values. The C=O bond lengths are slightly overestimated in the protonated compounds. Hydrogen bonding in the solid state contributes to the elongation of the O–H bond and shortening of the C=O bond compared to the gas-phase structures.

Reactions of benzaldehyde (**4**) with SbF_5 in aHF yielded the $[SbF_6]^-$ salt of the hemiprotonated, hydrogen-bridged dimeric [**4**–H–**4**]$^+$, even when a one molar equivalent of SbF_5 was used [Eq. (4)]. No evidence for the monoprotonated [**4**–H]$^+$ cation was obtained. Reacting acetaldehyde (**5**) with SbF_5 in 2:1 and 1:1 molar ratios, the [**5**–H–**5**]$^+$ and [**5**–H]$^+$ cations were isolated, respectively, in the solid state as the $[SbF_6]^-$ salts [Eq. (4) and (5)]. The three salts, [**4**–H–**4**][SbF_6], [**5**–H–**5**][SbF_6], and [**5**–H][SbF_6], were isolated as white powders and characterized by Raman spectroscopy at low temperature proving to be unstable, decomposing upon warming to RT. The [**5**–H–**5**][SbF_6] salt was only obtained in admixture with [**5**–H][SbF_6].

$$SbF_5 + 2\,O{=}CH(R) + HF \xrightarrow{aHF} [H(O{=}CHR)_2][SbF_6] \quad (R = C_6H_5\,(\mathbf{4}),\ CH_3\,(\mathbf{5})) \qquad (4)$$

$$SbF_5 + O{=}CH(CH_3) + HF \xrightarrow{aHF} [HO{=}CH(CH_3)][SbF_6] \qquad (5)$$

The X-ray crystal structures of the $[SbF_6]^-$ salts of hemiprotonated aldehydes [**4**–H–**4**][SbF_6] and [**5**–H–**5**][SbF_6] reveal the hydrogen-bridged dimeric nature of the oxonium cations (Figure 2), which contrasts that of the protonated ketones. Hydrogen-bridged dimeric cations were previously observed by X-ray crystallography for benzannelated 2-hydroxyhomotropylium[3] and [H(benzophenone)$_2$]$^+$ cations,[4] as well as for acetone, according to IR spectroscopy.[15] The cations [**4**–H–**4**]$^+$ and [**5**–H–**5**] are isolated, having no contacts with the anions in the unit cell. Cation [**4**–H–**4**]$^+$ is comprised of two symmetry-related hydrogen-bridged benzaldehyde molecules (O(1)–H(1) 1.213(3) Å, O(1)---O(1A) 2.425(4) Å). The previously synthesized [H(benzophenone)$_2$]$^+$ cation shows a similar O---O distance (2.470(3) Å) to **4**, however, the O–H–O moiety is asymmetric in the crystal structure.[4] Upon hemiprotonation of benzaldehyde, the C=O bond distance increases ([**4**–H–**4**]$^+$ 1.248(3) Å; **4** 1.212(3) Å) and the $C_{C=O}$–C bond length decreases ([**4**–H–**4**]$^+$ 1.441(4) Å) when compared to the reported structural data for **4** (1.479(4) Å) (Table 2).[16] Geometry optimization reproduced the planar geometry of [**4**–H–**4**]$^+$ and the *E*-configuration of the C=O–H moiety; the hydrogen-bridge is shown to be asymmetrical in the gas phase, whereas the symmetric hydrogen bridge in the crystal structure is imposed by crystallographic symmetry. The calculated C=O bond distances (1.256 and 1.246 Å) compare well with the experimental value for [**4**–H–**4**]$^+$, whereas the C–C bond distances are underestimated by the calculations (by up to 0.018 Å), likely due to packing effects in the solid state.

The crystal structure of [**5**–H–**5**][SbF_6] contains a protonated acetaldehyde in the *Z*-configuration that is hydrogen-bonded to a second acetaldehyde molecule in an *E*-configuration relative to its methyl group. The configuration of the lowest-energy gas-phase geometry of [**5**–H–**5**]$^+$ is the reverse, suggesting packing effects influence the configuration in the solid state. The *Z*-geometry of the oxonium cation [**5**–H]$^+$ was calculated to be only 3 kJ/mol higher in energy than *E*-[**5**–H]$^+$.

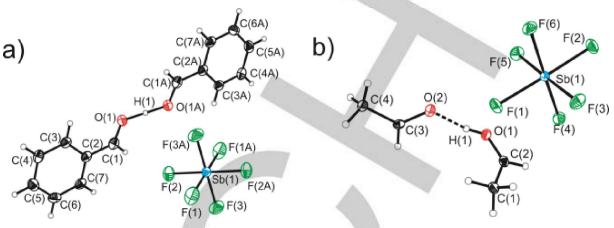

Figure 2. Thermal ellipsoid plots of a) [**4**–H–**4**][SbF_6] and b) [**5**–H–**5**][SbF_6]. Thermal ellipsoids are set at the 50% probability level.

The hydrogen-bond in [**5**–H–**5**]$^+$ is asymmetric, which contrasts with the symmetric hydrogen-bridge in [**4**–H–**4**]$^+$. The latter results in a significantly stronger bridging interaction in [**4**–H–**4**]$^+$. Similar to **1**–**4**, the C=O bond distance decreases ([**5**–H–**5**]$^+$ C(2)–O(1) 1.239(2) Å; **5** 1.208(3) Å) and the $C_{C=O}$–C bond increases ([**5**–H–**5**]$^+$ C(2)–C(1) 1.457(3) Å; **5** 1.514(5) Å) upon protonation (Table 2).[17] Interestingly, the second acetaldehyde appears to be almost equally affected by the hydrogen-bridge. The small difference in C=O bond lengths in the two acetaldehyde moieties is reproduced by the geometry optimization.

Table 2. Selected Experimental and Calculated Bond Lengths (Å) of Oxonium Cations [**4**–H–**4**]$^+$ and [**5**–H–**5**]$^+$, as well as the Parent Aldehydes Benzaldehyde (**4**) and Acetaldehyde (**5**).

	4		[**4**–H–**4**]$^+$	
	exptl [a]	*calcd* [c]	*Exptl*	*calcd* [c]
C=O	1.20936	1.208	1.248(3)	1.256, 1.246
C–C	1.47768	1.478	1.441(4)	1.423, 1.433
O–H			1.213(3)	1.140, 1.276
O---O			2.425(4)	2.415
	5		[**5**–H–**5**]$^+$	
	exptl [b]	*calcd* [d]	*Exptl*	*calcd* [d]
C=O	1.208(3)	1.205	1.239(2) C(2)–O(1)	1.240
			1.232(2) C(3)–O(2)	1.233
C–C	1.514(5)	1.501	1.457(3) C(2)–C(1)	1.464
			1.471(3) C(3)–C(4)	1.472
O–H			0.88(4), 1.58(4)	1.167, 1.253
O---O			2.4449(19)	2.419

[a] from Ref. 16; [b] from Ref. 17; [c] DFT calculations at the B3LYP/cc-pVTZ level of theory. [d] DFT calculations at the B3LYP/aug-cc-pVTZ level of theory.

The low-temperature Raman spectra of the protonated ketone and aldehyde salts were recorded at −100 °C (see Supporting Information), and vibrational frequencies of the geometry-optimized structures were calculated and used to aid in the assignments of the Raman bands. Protonation of the ketones is accompanied by a dramatic decrease in the characteristic C=O stretching frequency. For [**1**–H]$^+$, [**2**–H]$^+$, and [**3**–H]$^+$, the C=O stretching frequencies decrease between 116 and 155 cm^{-1} relative to the neutral parent compounds (Table 3), which is in agreement with a previous LT-IR study of [**3**–H][SbF_6].[15] This reflects a weakening of the C=O bond. DFT calculations

overestimate the decrease in the C=O stretching frequencies upon protonation (194 to 224 cm^{-1}), consistent with the absence of H-bonding in the computed gas-phase structures.

Unlike the protonated ketones, the C=O stretching frequency of [**4**–H–**4**][SbF_6] (1639 cm^{-1}) only decreases by 59 cm^{-1} relative to **4**. The Raman spectrum of [**5**–H–**5**][SbF_6] shows two C=O stretching frequencies (1665 and 1629 cm^{-1}), which are associated with protonated and H-bond accepting acetaldehyde moieties, respectively, observed in the crystal structure of [**5**–H–**5**][SbF_6]. As expected, the decreases in C=O stretching frequency is more dramatic for the monoprotonated acetaldehyde cation [**5**–H]$^+$ (108 cm^{-1}).

Table 3. Observed and Calculated ν(CO) Frequencies (cm^{-1}) for Protonated Ketones and Aldehydes.

	exptl [a]	*calcd* [b]
1	1719(13)	1779(17)[280]
[**1**–H]$^+$	1564(11)	1555(8)[184]
2	1743(16) 1727(23)	1806(15)[264]
[**2**–H]$^+$	1605(16)	1591(9)[211]
3	1751(3) 1709(16)	1782(13)[195]
[**3**–H]$^+$	1593(10) [c]	1588(4)[97]
4	1698(46)	1767(113)[287] [c] 1712(11)[23], [c]
[**4**–H]$^+$	1639(66)	1678(125)[61] [c]
5	1732sh 1712(33)	1805(13)[197]
[**5**–H–**5**]$^+$	1665(15) 1629(18)	1740(7)[117] 1715(15)[51]
[**5**–H]$^+$	1604(18)	1644(7)[137]

[a] Raman intensities, in $Å^4\ u^{-1}$, are given in parentheses. [b] DFT calculations at the B3LYP/aug-cc-pVTZ level of theory. Unscaled Raman intensities, in $Å^4\ u^{-1}$, are given in parentheses; infrared intensities, in km mol^{-1}, are given in square brackets; [c] Previous LT-IR study from Ref. 15 shows ν(CO) 1590 cm^{-1}; [d] DFT calculations at the B3LYP/cc-pVTZ level of theory.

Natural bond order (NBO) analyses were carried out to investigate the bonding in these protonated ketones and aldehydes (Supporting Information, Tables S18–S22). For acetone, the NPA charge on the carbonyl carbon increases from 0.59 to 0.73 when protonated, while the charge on oxygen does not change appreciably, suggesting that the hydroxycarbenium resonance structure (Scheme 1) cannot be neglected. The energy of the LUMO is dramatically lowered from −18 kJ/mol to −189 kJ/mol, making acetone more accessible for nucleophilic attack upon protonation, reflecting the increased reactivity of protonated carbonyl compounds as proposed intermediates in acid-catalyzed reactions. There is also a substantial decrease in the energy of the HOMO from −162 kJ/mol to −376 kJ/mol, reducing the accessibility to electrophilic attack upon forming the O–H bond. When protonated, the C=O bond order in acetone decreases from 1.83 to 1.39 (Table 4), reflecting the significant weakening of the bond, which is paralleled by the increase in C=O bond length and lowering of the C=O stretching frequency. Similar trends are found for the cyclopentanone and 2-adamantanone systems. NBO analyses for **5**, [**5**–H]$^+$, and [**5**–H–**5**]$^+$ showed the expected decrease in the C=O bond order from **5** (1.88) to protonated acetaldehyde [**5**–H]$^+$ (1.47), with that of hemiprotonated [**5**–H–**5**]$^+$ being intermediate (1.61 and 1.65) (Table 4).

Table 4. Selected NPA Charges, Valences and Wiberg Bond Indices of Cations [**3**–H]$^+$, [**5**–H–**5**]$^+$, [**5**–H]$^+$, and their Parent Compounds Acetone (**3**) and Acetaldehyde (**5**).

	NPA Charges (Valence [a]*)*	*NPA Charges (Valence* [a]*)*	*Wiberg Bond Indices*
	O	C	CO
3	−0.55 (2.04)	0.59 (3.87)	1.83
[**3**–H]$^+$	−0.52 (2.23)	0.73 (3.71)	1.39
5	−0.52 (2.06)	0.44 (3.83)	1.88
[**5**–H]$^+$	−0.49 (2.26)	0.57 (3.61)	1.47
[**5**–H–**5**]$^+$	−0.52 (2.20)	0.54 (3.84)	1.61
	−0.55 (2.17)	0.53 (3.70)	1.65

[a] Sum of the Wiberg Bond Indices per atom.

The NPA charge on the carbon of the carbonyl in **5** is 0.44 and increases to 0.57 in [**5**–H]$^+$. The effect is slightly smaller in [**5**–H–**5**]$^+$ where the charges are 0.53 and 0.54. A similar trend is observed between benzaldehyde and the hemiprotonated cation [**4**–H–**4**]$^+$.

In conclusion, the cations presented in this study are the first examples of representative protonated ketones and aldehydes to be isolated and structurally characterized in the solid state. As a result, the presented experimental and computational results provide key data about a class of intermediates that are ubiquitous in acid-catalysed organic reaction mechanisms. Protonation significantly increases the electrophilicity of the carbonyl carbon, as reflected by bond elongation, significant decrease in the ν(CO) stretching frequencies, as well as calculated charges, bond orders, and LUMO energies.

Acknowledgements

We thank the Natural Scienes and Engineering Research Council of Canada (NSERC) for funding this research (Discovery Grants for M.G. and S.D.W.). Computational studies were performed using equipment funded through the Canada Foundation of Innovation, as well as resources made available through Westgrid and Compute/Calcul Canada

Keywords: density functional calculations • oxonium cation • reactive intermediates • superacidic systems • X-ray diffraction

[1] a) T. Birchall, R. J. Gillespie, *Can. J. Chem.* **1965**, *43*, 1045–1051; b) G. A. Olah, M. Calin, *J. Am Chem Soc.* **1968**, *90*, 938–943; c) G. A. Olah, D. H. O'Brien, M. Calin, *J. Am Chem Soc.* **1967**, *89*, 3582–3586; d) G. A. Olah, D. H. O'Brien, M. Calin, *J. Am Chem Soc.* **1967**, *89*, 3586–3590; e) G. A. Olah, G. Liang, G. D. Mateescu, *J. Org. Chem.* **1974**, *39*, 3750–3754; f) G. A. Olah, Y. Halpern, Y. K. Mo, G. Liang, *J. Am Chem Soc.* **1972**, *94*, 3554–3561.

[2] a) R. F. Childs, A. Varadarajan, C. J. L. Lock, R. Faggiani, C. A. Fyfe, R. E. Wasylishen, *J. Am Chem Soc.* **1982**, *104*, 2452–2456; b) R. F. Childs, R. Faggiani, C. J. L. Lock, M. Mahendran, S. D. Zweep, *J. Am Chem Soc.* **1986**, *108*, 1692–1693; c) S. K. Chadda, R. F. Childs, R. Faggiani, C. J. L. Lock, *J. Am Chem Soc.* **1986**, *108*, 1694–1695; d) R. F. Childs, M. D. Kostyk, C. J. L. Lock, M. Mahendran, *J. Am Chem Soc.* **1990**, *112*, 8912–8920.

[3] R. F. Childs, R. Faggiani, C. J. L. Lock, A. Varadarajan, *Acta Crystallogr. Sect. C* **1984**, *40*, 1291−1294.

[4] D. Stasko, S. P. Hoffmann, K. C. Kim, N. L. P. Fackler, A. S. Larsen, T. Drovetskaya, F. S. Tham, C. A. Reed, C. E. F. Rickard, P. D. W. Boyd, E. S. Stoyanov, *J. Am Chem Soc.*, **2002**, *124*, 13869−13876.

[5] A. K. Chandra, M. T. Nguyen, T. Zeegers-Huyskens, *Chem Phys.* **2000**, *255*, 149−163.

[6] V. Aviyente, T. Vernali, *J. Mol. Struc. (Theochem)* **1992**, *277*, 285−292; b) V. Aviyente, M. Iraqi, T. Peres, C. Lifshitz, *J. Am. Soc. Mass Spectrom* **1991**, *2*, 113−119.

[7] a) H. Lampert, W. Mikenda, A. Karpfen, *J. Phys. Chem. A.* **1997**, *101*, 2254−2263; b) S. Chakraborty, A. Patzer, O. Dopfer, *J. Chem. Phys.* **2010**, *133*, 044307/1−044307/12.

[8] I. Alata, R. Omidyan, C. Dedonder-Lardeux, M. Broquier, C. Jouvet, *Phys. Chem. Chem. Phys.* **2009**, *11*, 11479−11486.

[9] a) A. T. Hagler, Z. Karpas, F. S. Klein, *J. Am. Chem. Soc.* **1979**, *101*, 2191−2196; b) W. B. Tzeng, S. Wei, A. W. Castleman Jr. *Chem. Phys. Lett.* **1990**, *168*, 30−36.

[10] R. Minkwitz, S. Schneider, H. Preut, *Angew. Chem. Int. Ed.* **1998**, *37*, 494−496.

[11] J. P. Amoureux, M. Bee, *J. Phys. C.* **1980**, *13*, 3577−3583.

[12] D. S. Yufit, J. A. K. Howard, *Acta. Crystallogr. Sect. C* **2011**, *67*, 104−106.

[13] D. R. Allan, S. J. Clark, R. M. Ibberson, S. Parsons, C. R. Pulham, L. Sawyer, *Chem. Commun.* **1999**, 751−752.

[14] F. H. Allen, O. Kennard, D. G. Watson, L. Brammer, A. G. Orpen and R. Taylor in *International Tables for Crystallography*, *Vol.* C (Eds.: A. J. C. Wilson), Kluwer Academic, Dordrecht, **2006**, pp. 685–706.

[15] P. V. Huong, G. Noel, *Spectrochim Acta, Part A*, **1976**, *32A*, 831–835.

[16] C. Kato, S. Konaka, T. Iijima, M. Kimura, *Bull. Chem. Soc. Jpn.* **1969**, *42*, 2148−2158.

[17] K. B. Borisenko, C. W. Bock, I. Hargittai, *J. Phys. Chem.* **1996**, *100*, 7426−7434.

Entry for the Table of Contents (Please choose one layout)

Layout 1:

COMMUNICATION

Text for Table of Contents

D. Stuart, S. D. Wetmore, and M. Gerken

Page No. – Page No.

Solid-state Structure of Protonated Ketones and Aldehydes

Layout 2:

COMMUNICATION

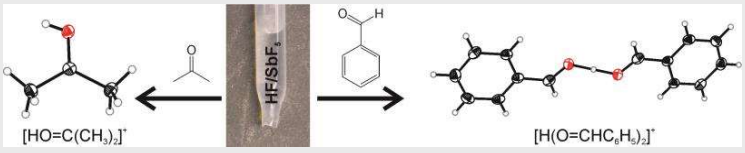

Daniel Stuart, Prof. Dr. Stacey D. Wetmore, Prof. Dr. Michael Gerken

Page No. – Page No.

Solid-State Structure of Protonated Ketones and Aldehydes

Structures of Reactive Intermediates: Solid-state structures of protonated carbonyl compounds are presented. Whereas protonation of ketones (acetone, cyclopentanone and adamantanone) in superacidic solution yielded the mononuclear oxonium ions, hemiprotonated hydrogen-bridged dinculear structures were observed in the crystal structure obtained from reactions of benzaldehyde or acetaldehyde with HF/SbF_5.